frontiers | Frontiers in Physics

ORIGINAL RESEARCH
published: 14 April 2022
doi: 10.3389/fphy.2022.836977

Hydrocarbon Charge History of the Upper Paleozoic, Ordos Basin as Revealed by Fluid Inclusions

Qing Cao[1], Xinshan Wei[2], Zhangxing Chen[3], Jingzhou Zhao[1] and Mingju Tang[1]*

[1]Shaanxi Key Laboratory of Petroleum Accumulation Geology, Xi'an Shiyou University, Xi'an, China, [2]PetroChina Company Limited Changqing Oilfield Branch, Xi'an, China, [3]Reservoir Simulation Group, University of Calgary, Calgary, AB, Canada

The petrographic characteristics of fluid inclusions of the main gas-bearing intervals of the Upper Paleozoic in the Ordos Basin are analyzed by means of plane-polarized light, fluorescence microscopy, and microthermometry. With the burial history of the basin, the charging and enrichment of natural gas in low-permeability reservoirs are also studied through a comparison of parameters such as the homogenization temperature and freezing temperature of aqueous inclusions associated with hydrocarbon inclusions. A comprehensive analysis of the assemblage characteristics, components, and temperature of fluid inclusions of the Upper Paleozoic shows that the abundance, attitude, and composition of gaseous hydrocarbon inclusions can reflect petroleum enrichment in low-permeability reservoirs. The homogenization temperature and freezing temperature of aqueous inclusions associated with gaseous hydrocarbon inclusions show no obvious discontinuities, indicating that natural gas charging was a long and continuous process since the Late Triassic to Early Cretaceous (210–100 Ma) and natural gas accumulation mainly occurred during the Early Cretaceous (125–100 Ma).

Keywords: fluid inclusion, tight sandstone reservoir, gas charge history, upper paleozoic, ordos basin

OPEN ACCESS

Edited by:
Qingxiang Meng,
Hohai University, China

Reviewed by:
Zhengjian Xu,
Chongqing University of Science and Technology, China
Hong Li,
Northwest University, China

****Correspondence:***
Qing Cao
caoqing@xsyu.edu.cn

Specialty section:
This article was submitted to Interdisciplinary Physics, a section of the journal Frontiers in Physics

Received: *16 December 2021*
Accepted: *25 March 2022*
Published: *14 April 2022*

Citation:
Cao Q, Wei X, Chen Z, Zhao J and Tang M (2022) Hydrocarbon Charge History of the Upper Paleozoic, Ordos Basin as Revealed by Fluid Inclusions. Front. Phys. 10:836977. doi: 10.3389/fphy.2022.836977

INTRODUCTION

Fluid inclusions in different types of minerals can provide information on the paleo-pressure, paleo-temperature, and composition of reservoir fluids (aqueous, oil, and gas) included within sediments during burial. Information on a reservoir fluid can be obtained from studies of fluid inclusions trapped within minerals formed during geothermal activities. Different types of fluid inclusions have been researched to determine: 1) the evolution of reservoir temperature and pressure [1]; 2) the geological timing of petroleum migration and petroleum accumulation, such as petroleum source and types, paleohydrocarbon-water contact, and migration pathways [2]; and 3) the evolution of grains containing oil inclusion and fluid salinity [3]. PT phase diagrams of reservoir fluids can be rebuilt based on the isochore calculated using pressure-temperature data, which can be obtained from fluid inclusions. The evolution of not only pressure-temperature conditions but also hydrocarbons in the reservoir can be surmised from hydrocarbon inclusions in different assemblages, in which hydrocarbons are trapped in different inclusion assemblages during burial [4, 5].

Increasingly more testing techniques are being applied to analyze hydrocarbons, such as UV fluorescence, fluorescence spectroscopy, micro-laser Raman spectroscopy, and gas chromatography-carbon Isotope mass spectrometry. Fluid inclusions are trapped in different growth zones or healed micro-fractures, which are the basis of identifying fluid inclusion assemblages [6]. According to the simultaneity of the formation of inclusions and their direct host minerals, the approach that a

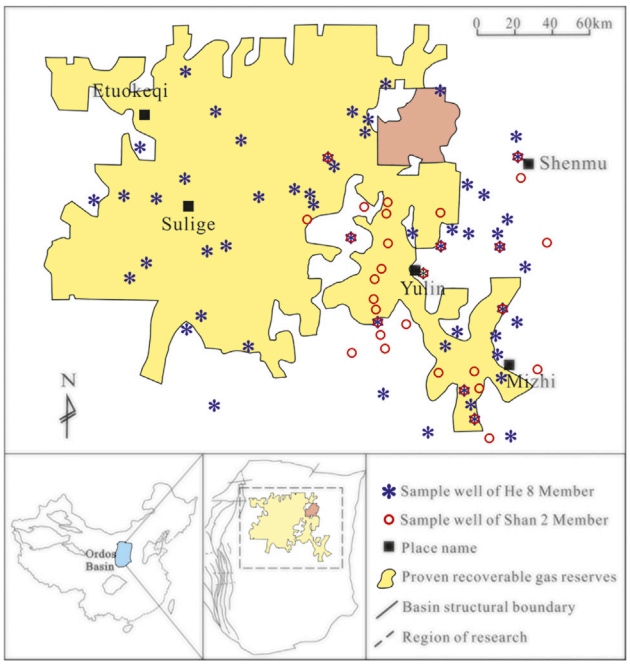

FIGURE 1 | Division of tectonic units and location of the samples.

sequence of diagenetic authigenic minerals is the fundamental basis of determining the periods and times of inclusions in sedimentary rocks has been brought forward from the viewpoint of crystallography and mineralogical mechanisms of inclusion formation within a single healed micro-fracture [7, 8].

The classifications of the petroleum charging history in tight sandstone gas reservoirs of the Ordos Basin are divergent due to differences in the principles of estimation and division. There are three opinions at present: One period, the conclusions of which are based on a single peak of homogenization temperature [9]; two periods, which can be summarized by twin peaks of homogenization temperatures [10]; and three periods and above, the conclusions of which are mainly summed from homogenization temperature ranges and evolution of thermal burial history [11]. Multiple opinions exist for the same reservoir because of not only the small amount of temperature data but also less assemblage analysis associated with the diagenetic sequence. All inclusion temperatures could be used to analyze the diagenetic process, but only the temperature tested for aqueous inclusions specially associated with hydrocarbon inclusions can be used to rebuild the gas charge history.

GEOLOGIC SETTING

Five large tight sandstone gas fields with over 100 billion proven reserves of coalbed methane, namely Sulige, Jingbian, Yulin, Zizhou, and Shenmu, have been found in the Ordos basin (**Figure 1**). Meanwhile, the terms of trapping mechanism of these large gas fields have been identified from lithological accumulations to continuous accumulations [12]. The latest enrichment law of gas accumulation has suggested that it is closer to a "Quasi-continuous accumulation model" [13].

Gas source rocks in the upper Paleozoic of the Ordos Basin have shown "large-covered hydrocarbon generation" and "continuous gas accumulation" gas supply characteristics; organic matter maturity in the major part in the central basin reached the thermal-cracking condensate-generation stage and dry gas generation stage. Natural gas was mainly generated throughout the period from the middle Jurassic to Early Cretaceous, and the gas generation intensity surpassed 10×10^8 m^3/km^2, accounting for over 85% of the basin area. The main gas-bearing intervals of the basin in the Upper Paleozoic are lithic quartz sandstone of the He 8 Member (bottom of the Shihezi Formation) in the Sulige area and quartz sandstone of the Shan 2 Member (bottom of the Shanxi Formation) in the Yulin area. The gas-bearing sandstone reservoirs of the He 8 and Shan 2 Members are generally tight, and their average porosities are 8.4 and 8.3%, respectively, with median permeability values of 0.58×10^{-3} μm^2 and 0.59×10^{-3} μm^2, respectively. The Upper Paleozoic coal-bearing source rocks are located a distance of less than 30 m from the gas-bearing quartz sandstone of the Shan 2 Member, and between 80 and 130 m from the gas-bearing lithic quartz sandstone of the He 8 Member. Due to the relatively short transport distance between source rocks and reservoirs and the good preservation conditions, the natural gas migration and the charging process can be considered a process of enrichment and accumulation.

METHODS AND SAMPLES

All types of tests on fluid inclusions were implemented in the Shaanxi Key Laboratory of Petroleum Accumulation Geology. Several instruments, such as ZEISS transmission light-fluorescence microscope (Axioskop 40, Germany), Renshaw inVia laser Raman spectrometer (514.5 nm wavelength, United Kingdom), Elementar gas chromatography-carbon Isotope mass spectrometer (Isoprime 100, Germany), and Linkam heating-freezing stage (THMS 600G, United Kingdom), were used in the tests. The testing procedures and technical requirements are based on the China Oil and Gas Industry Standard of "Microscopic Temperature Measurements of Fluid Inclusions in Sedimentary Basins (SY/T6010-2011, PRC)" and "Analysis of natural gas Composition-Laser Raman spectroscopy (SY/T 7433-2018, PRC)".

For tests on the fluid inclusion geochemistry characteristics and their significance, 120 samples were collected from 76 wells in the central part in the Ordos Basin (**Figure 1**). Fluid inclusions trapped in quartz overgrowths and micro-fractures have been tested in detail as primary targets. On the basis of generalizing fluid inclusion types and their occurrences, fluid inclusions within the quartz overgrowth and healing micro-fractures were selected for temperature measurement. The selected sandstone grains were crushed in a vacuum closed tank after they had been cleaned, and then the gas in the tank was extracted through inclusion composition tests and carbon isotope analysis. The aqueous inclusions associated with hydrocarbon inclusions were emphatically tested. Combined with their geochemical parameters, the formation order of inclusions in different occurrences was

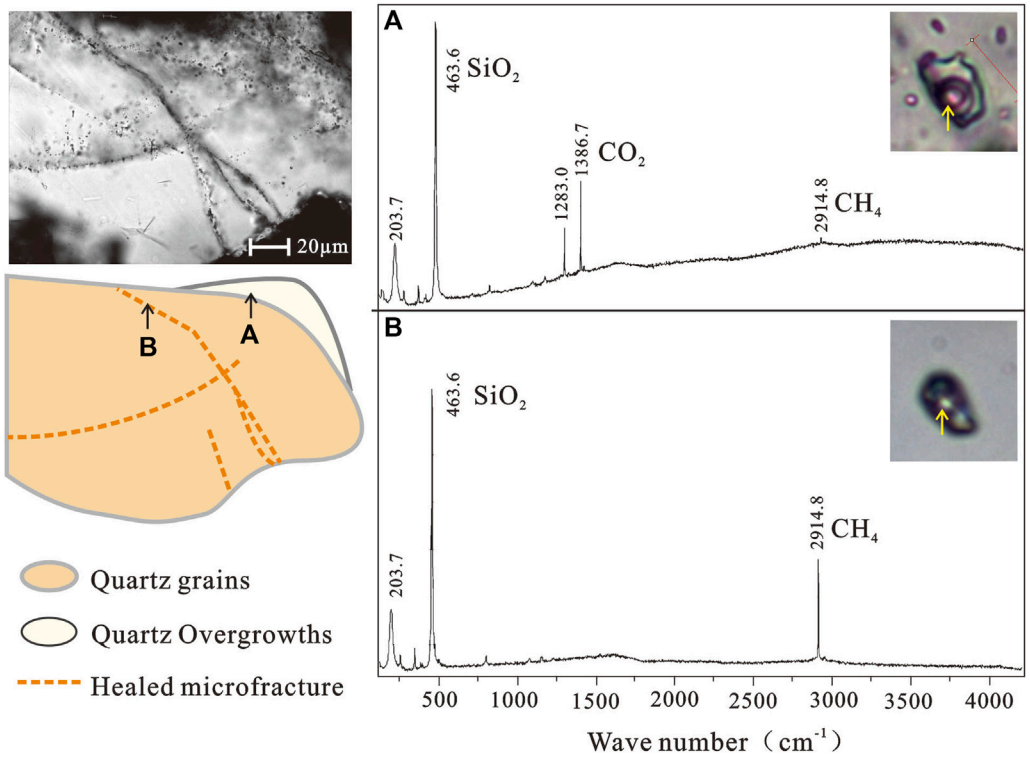

FIGURE 2 | Raman spectrogram of gaseous hydrocarbon inclusions (Mi-6, 2,638.4 m).

determined synthetically such that the charging status of natural gas in the Upper Paleozoic can be deduced accordingly.

RESULTS AND DISCUSSION

Petrography

The lithofacies characteristics of the fluid inclusions were systematically summarized by observing the transmission light of the microscope and fluorescence contrast. In this manner, inclusion assemblages were determined and the order for entrapment of different inclusion assemblages was restored. Accordingly, fluid inclusions within the quartz grains of the He 8 Member (bottom of the Shihezi Formation) and the Shanxi Formation in the central basin were divided into three categories:

1) Aqueous inclusions: Beadlike and ribbon-like distributed in quartz host minerals, mostly showing elliptic and irregular shapes. Most of the individual sizes are comparatively small at about 3–9 μm with a gas-liquid ratio of 5–10%. They became a homogeneous and pure liquid after heating.
2) Gaseous hydrocarbon inclusions: Mainly trapped in quartz overgrowth edges and healing micro-fractures, normally associated with a large number of aqueous inclusions, and beadlike distributed among the quartz host minerals. The individual sizes vary largely from 2 to 15 μm. They mostly show round, elliptic, and irregular shapes with a gas-liquid ratio varying from 20 to 80%. They are light gray–light brown under transmitted light and have no fluorescent display.
3) CO_2 inclusions: Mainly enriched with gaseous and liquid CO_2 in the Upper Paleozoic, which were primarily trapped in quartz overgrowth edges. The relative contents of CO_2 (gaseous and liquid) and liquid saline are slightly different in different areas.

Geochemistry Features

The gas-phase component analysis of inclusions is based on the determination of the inclusion assemblage characteristics, and different inclusions were selected for laser Raman spectroscopy. The results showed that the dominant compositions are CO_2 and CH_4. Inclusions trapped in quartz overgrowths were mostly composed of CO_2 (**Figure 2A**). Gaseous hydrocarbon-bearing inclusions trapped in quartz overgrowths were dominated by CO_2 and contained a small amount of CH_4. Gaseous hydrocarbon inclusions trapped in micro-fractures and with a gas-liquid ratio of over 50% were mostly composed of CH_4 (**Figure 2B**). With a gradual decrease in the CO_2 fraction in gas inclusions, the CH_4 fraction increases correspondingly.

The GC-MS test results suggested that CH_4 dry coefficients of inclusions within sandstone grains and sandstone pores showed a certain difference (**Figure 3A**). The CH_4 dry coefficient in gas reservoirs is higher than that in inclusions of the He 8 Member in the Sulige and Yulin gas fields, which means that the present gas reservoirs are mainly trapped throughout the charging and reforming of gas with different maturities. The CH_4 dry

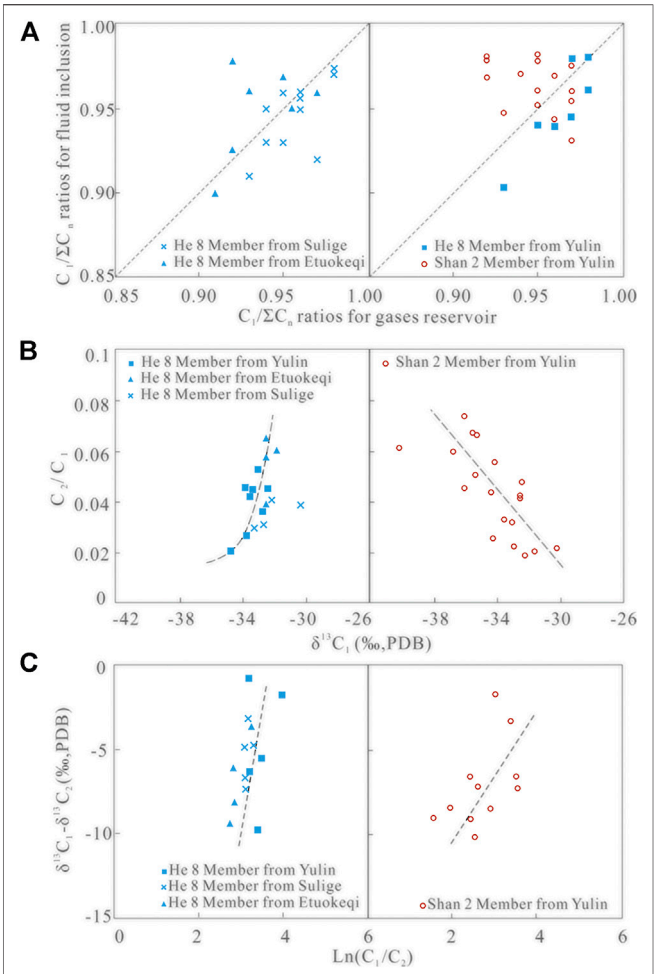

FIGURE 3 | Plot of geochemical features between gaseous inclusions and gas reservoirs.

coefficient in the gas reservoirs is lower than that in inclusions of the He 8 Member in the Eketuoqi area (western Sulige gas field), which may be caused by gas diffusion migration. The dry coefficients of these reservoirs does not exhibit obvious regularity of the Shan 2 Member in the Yulin gas field. The gaseous components and carbon isotopes of the gas inclusions in the main gas-bearing sandstones in the Yulin and Sulige areas suggest that the carbon isotopes of gaseous inclusions are generally lighter than those of the current gas reservoirs. There is a slight positive correlation between Ln (C_1/C_2) and $\delta^{13}C_1$-$\delta^{13}C_2$ in the Yulin area. The regularity indicates that the main trapped gas components and their carbon isotopes are controlled by the maturity of source rocks (**Figure 3B**). The GC-MS test results also show that the value of C_2/C_1 presented a concave curve shape and positive correlation with $\delta^{13}C_1$ in the Sulige gas field, which may be caused by gas migration. The value of C_2/C_1 is negatively correlated with $\delta^{13}C_1$ in the Yulin gas field, suggesting charging gas with different maturities (**Figure 3C**).

The hydrocarbon components of the gaseous inclusions in the study area can be used to semi-quantitatively analyze the enrichment status of natural gas in tight sandstone reservoirs. The gaseous components of the inclusion assemblage show that Natural gas enrichment in the Shan 2 Member in the Yulin area is mainly affected by source rock maturity. The natural gas enrichment in the He 8 Member (Sulige area) is dominated by source rock maturity, which is also influenced by diffusion and migration partially.

Fluid Inclusion Temperature

Based on the summary of the fluid inclusion types and their occurrences, fluid inclusions within quartz grains overgrowth edges and healing micro-fractures were selected for the temperature measurement. More than 1,400 temperature data sets of fluid inclusions of the He 8 Member and the Shanxi Formation were obtained. The results of the test showed that the homogenization temperature of aqueous inclusions ranged from 90 to 170°C, with an overall continuous and broad pattern. The mean homogenization temperature of the He 8 Member was 133°C and the median value was 138°C, while the homogenization temperature of the Shan 2 Member was 135°C and the median value was 136°C. The freezing temperature of the inclusions ranged from −2°C to −12°C and the corresponding homogenization temperature ranged from 120 to 165°C, showing a large difference in the freezing temperature of both reservoirs.

The initial melting temperature of aqueous inclusions of the He 8 Member and the Shanxi Formation were generally higher than −20.8°C, indicating that it is mainly a NaCl system solution. The freezing temperature of fluid inclusions ranged from −3°C to −13°C, and most inclusions were distributed between −4°C and −10°C. Freezing temperature was significantly correlated to the corresponding homogenization temperature. The freezing temperature of a small amount of secondary inclusions was distributed between −12°C and −15°C, which obviously deviates from the variation trend of most homogenization temperatures and freezing temperatures. At the same time, NaCl sub-crystals were observed in such high-salinity inclusions.

Fluid Inclusion Assemblage

The characteristics of fluid inclusion assemblages (FIAs) show obvious differences among different diagenetic periods. Based on these differences, the charging status of oil and gas in a reservoir can be analyzed, where different FIAs were trapped during different geological periods. According to the types of fluid inclusions, occurrences, temperature (homogenization temperature and freezing temperature) and other parameters, fluid inclusions of the He 8 Member and the Shanxi Formation can be divided into two types (**Figure 4**).

In order to better analyze the gas charging information obtained from the inclusions, further temperature measurements of the aqueous inclusions adjacent to hydrocarbon inclusions were taken under laser Raman microscopy. The statistical results showed that the homogenization temperatures of these aqueous inclusions associated with hydrocarbon inclusions are between 100 and 170°C (**Figure 5**). Its overall continuous and unimodal distribution indicates that the gas charging process recorded by the inclusions was a long and continuous process. Since the gas-liquid ratio of gaseous hydrocarbon inclusions indirectly

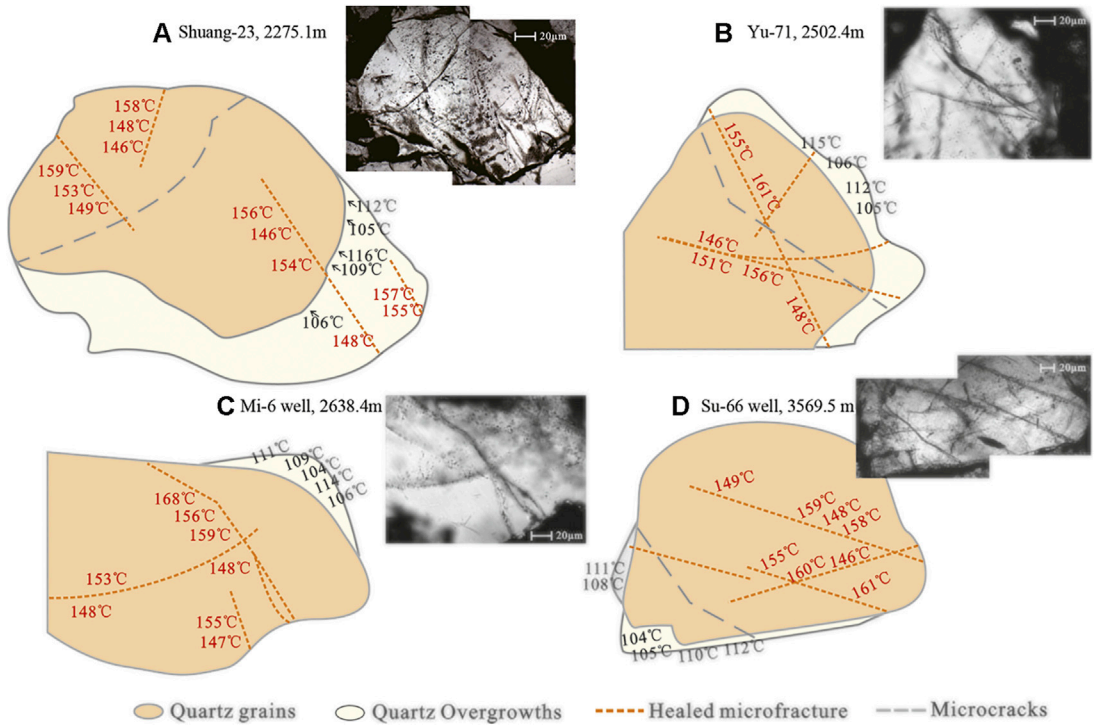

FIGURE 4 | Homogenization temperature of fluid inclusions in different FIAs.

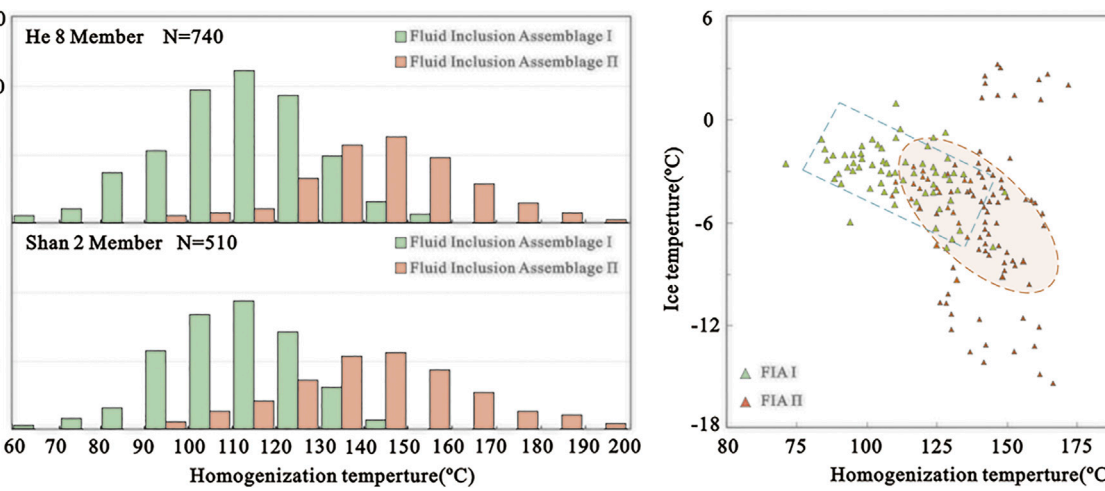

FIGURE 5 | Distribution of homogenization temperature in different FIAs in the Upper Paleozoic in Ordos Basin.

reflects the state of gas-water enrichment in sandstone reservoirs, gaseous hydrocarbon inclusions trapped in the micro-fractures are further classified according to the gas-liquid ratio. Inclusions with a relatively high gas-liquid ratio correspond to homogenization temperatures of 140–170°C, indicating relatively high enrichment of natural gas in a reservoir. A narrower temperature range indicates that inclusions were trapped within a relatively short time.

Constraints on Gas Charge History

On the basis of the lithofacies determination of the inclusions, the depth and burial history of inclusions were acquired from inclusion homogenization temperature and the paleo-geothermal history of the basin, and the state and time of natural gas charging were deduced by combining the geochemical composition of the inclusions (**Table 1**; **Figure 6**).

TABLE 1 | Combination features, geological significance, temperature range and estimation of trapping time of different FIAs.

No	Petrographic Relationship	Characteristic	Geologic Information	Temperature	Trapped Time	
					Sulige Area	Yulin Area
①	associated with gaseous hydrocarbon inclusion	1. All secondary inclusions in different occurrences; 2. Show associated relationship with gaseous hydrocarbon	Natural gas charging process records	90–170°C	225–100 Ma	225–100 Ma
②	Associated with FIA Ⅰ	1.Trapped in overgrowth; 2. Gaseous hydrocarbon inclusions with low gas-liquid ratio and low abundance; 3. Gaseous were dominated by CO_2	Natural gas initial charging. Diagenetic active period	100–125°C	210–140 Ma	210–140 Ma
③	Associated with FIA Ⅱ	1.Trapped in healing micro-fractures; 2. High gas-liquid ratio and high abundance; 3. Gaseous were dominated by CH_4	Natural gas continuously charging	125–170°C	140–100 Ma	140–100 Ma
④	associated with high gas-liquid ratio gaseous hydrocarbon inclusion	1.Trapped in healing micro-fractures; 2. Gas-liquid ratio over 50%; 3. Gaseous components were dominated by CH_4	Natural gas charging substantially main charging period	140–170°C	125–100 Ma	125–100 Ma

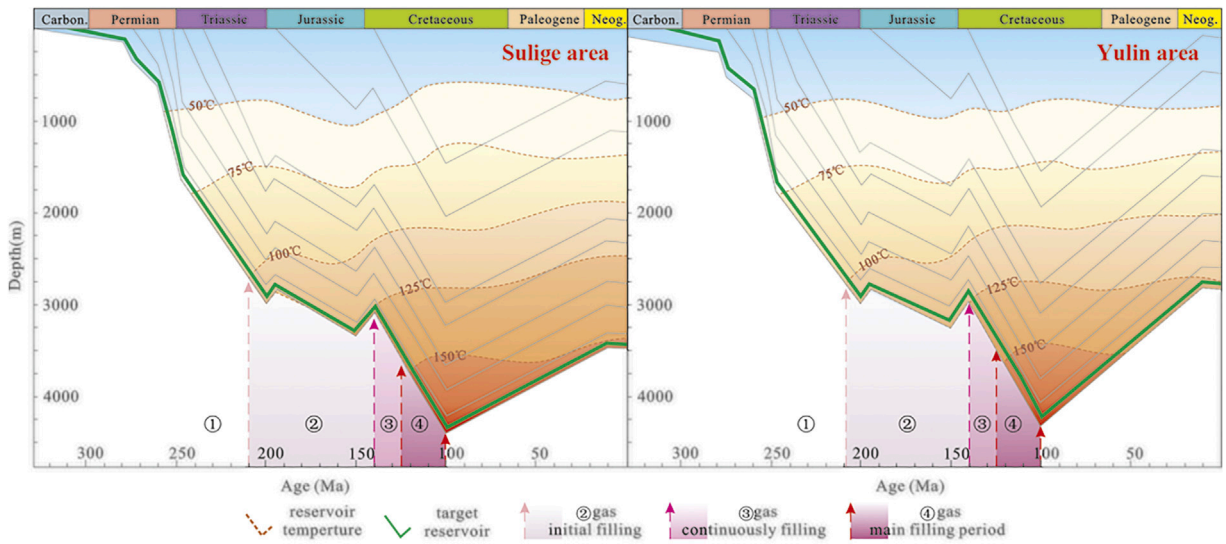

FIGURE 6 | The gas accumulation period based on the thermal history of Upper Paleozoic in Ordos Basin.

FIA Ⅰ: the laser Raman spectroscopy tests of these gaseous hydrocarbon inclusions showed that the components were dominated by CO_2 with a small amount of CH_4. The homogenization temperature of aqueous inclusions associated with these gaseous hydrocarbon inclusions ranges from 100 to 125°C; that is, natural gas charging occurred during the middle-late Jurassic to early Cretaceous (210–140 Ma). During this period, the Upper Paleozoic coal-bearing source rocks gradually began to generate and expel hydrocarbons. The small amount of originally generated low-maturity natural gas was expulsed into the adjacent reservoirs and thus the abundance and CH_4 content of the trapped gas hydrocarbon inclusions were low (**Table 1**①+②, **Figure 6**).

FIA Ⅱ: the laser Raman spectroscopy tests of these gaseous hydrocarbon inclusions showed that the gas components were dominated by CH_4. The homogenization temperature of aqueous inclusions associated with these gaseous hydrocarbon inclusions ranges from 125 to 170°C. The homogenization temperature of aqueous inclusions conspicuously associated with gaseous hydrocarbon inclusions having large gas-liquid ratio ranges from 140 to 170°C, indicating that the charging time of natural gas was the Early Cretaceous (140–100 Ma). During this period, the hydrocarbon source rocks reached the peak of gas expulsion in their evolutionary history. The source rocks expelled considerable highly matured natural gas and were enriched in the adjacent tight sandstones. Therefore, the trapped gas hydrocarbon inclusions have high abundance and high CH_4 content, indicating that this period was the main charging period of natural gas of the Upper Paleozoic (**Table 1**③+④, **Figure 6**).

The homogenization temperatures of aqueous inclusions (trapped in FIA-Ⅰ and FIA-Ⅱ) in the gas-bearing reservoirs of the Upper Paleozoic show no obvious discontinuities (100–170°C),

indicating that the gas charging history was a relatively long and continuous process, which continued from the Middle Jurassic to Early Cretaceous (210–100 Ma). However, the relatively high gas-liquid ratio of hydrocarbon inclusions indirectly reflects the state of gas-water accumulation in the reservoirs, and the homogenization temperature range of adjacent aqueous inclusions is relatively narrow (140–170°C), i.e., the Early Cretaceous (125–100 Ma) was the main charging period (**Table 1④**, **Figure 6**).

CONCLUSION

1) According to the characteristics of hydrocarbon inclusion assemblages, geochemical component parameters of inclusions, homogenization temperature, and freezing temperature, fluid inclusions in the quartz grains of the He 8 Member and Shan 2 Members in the Ordos Basin can be classified into two types: FIA Ⅰ and FIA Ⅱ. FIA Ⅰ has low gaseous hydrocarbon abundance and low gas-liquid ratio. Its gas components are dominated by CO_2 with a small amount of CH_4. The high abundance of aqueous inclusions suggest that an active water-rock interaction occurred during that period. The gaseous hydrocarbon inclusions indicate the initial status of natural gas charging. FIA Ⅱ contains a large amount of CH_4, with high gaseous hydrocarbon abundance and high gas-liquid ratio, indicating the main gas charging and accumulation within the tight reservoirs.
2) There was no clear cutoff in the test temperature (homogenization temperature and freezing temperature), which means the gas charging history was a long and continuous process since Late Triassic to Early Cretaceous (210–100 Ma); in the meantime, the occurrence of gaseous hydrocarbon inclusions with a high gas-liquid ratio and the temperature of the associated aqueous inclusions indicated that the main accumulation period of natural gas was the Early Cretaceous (125–100 Ma).

DATA AVAILABILITY STATEMENT

The original contributions presented in the study are included in the article/Supplementary Materials, further inquiries can be directed to the corresponding author.

AUTHOR CONTRIBUTIONS

QC: Conceptualization, resources, data curation, analysis, writing, review, editing. XW: review, editing. ZC: review, editing. JZ: supervision. MT: data curation.

FUNDING

This work was financially supported by Scientific Research Program Funded by Shaanxi Provincial Education Department (Program No. 2017JS111).

REFERENCES

1. Aplin AC, Larter SR, Bigge MA, Macleod G, Swarbrick RE, Grunberger D. PVTX History of the North Sea's Judy Oilfield. *J Geochemical Exploration* (2000) 69-70:641–4. doi:10.1016/s0375-6742(00)00066-2
2. Rezaee M, Tingate PR. Origin of Quartz Cement in Tirrawarra Sandstone, Southern cooper basin, South Australia. *J Sediment Res* (1997) 67:168–77. doi:10.1306/D4268522-2B26-11D7-8648000102C1865D
3. Burruss RC. Diagenetic Palaeotemperatures from Aqueous Fluid Inclusions: Re-equilibration of Inclusions in Carbonate Cements by Burial Heating. *Mineral Mag* (1987) 51:477–81. doi:10.1180/minmag.1987.051.362.02
4. Cao Q, Zhao JZ, Zhao XH. Characteristics and Significance of Fluid Inclusions from Majiagou Formation, Yichuan- Huangling Area, Ordos basin. *Adv Earth Sci* (2013) 28(7):819–28. doi:10.11867/j.issn.1001-8166.2013.07.0819
5. Ren D, Ma L, Liu D, Tao J, Liu X, Zhang R. Control Mechanism and Parameter Simulation of Oil-Water Properties on Spontaneous Imbibition Efficiency of Tight Sandstone Reservoir. *Front Phys* (2022) 10:829763. doi:10.3389/fphy.2022.829763
6. Xu Z, Liu L, Liu B, Wang T, Zhang Z, Wu K, et al. Geochemical Characteristics of the Triassic Chang 7 Lacustrine Source Rocks, Ordos Basin, China: Implications for Paleoenvironment, Petroleum Potential and Tight Oil Occurrence. *J Asian Earth Sci* (2019) 178:112–38. doi:10.1016/j.jseaes.2018.03.005
7. Tao SZ. Sequence of Diagenetic Authigenic mineral the Basis of Timing the Inclusions Formation in Sedimentary Rocks. *Pet Exploration Development* (2006) 33:154–60. doi:10.3321/j.issn:1000-0747.2006.02.007
8. Chen Y, Wang X, Bodnar RJ. UV Raman Spectroscopy of Hydrocarbon-Bearing Inclusions in Rock Salt from the Dongying Sag, Eastern China. *Org Geochem* (2016) 101:63–71. doi:10.1016/j.orggeochem.2016.08.010
9. Liu JZ, Chen HH, Li J, Hu G-y, Shan X-q. Using Fluid Inclusion of Reservoir to Determine Hydrocarbon Charging Orders and Times in the Upper Paleozoic of Ordos basin. *Geol Sci Technology Inf* (2005) 24(4):60–6. doi:10.3969/j.issn.1000-7849.2005.04.011
10. Zhang WZ, Guo YR, Tang DZ, Junfeng Z, Ming L, Hao X, et al. Characteristics of Fluid Inclusions and Determination of Gas Accumulation Period in the Upper Paleozoic Reservoirs of Sulige Gas Field. *Acta Petrolei Sinica* (2009) 30(5):685–91. doi:10.7623/syxb200905009
11. Li XQ, Li J, Wang KD. Charging Migration and Accumulation Characteristics of Natural Gas in Sulige Low Permeability sandstone Large Gas Field. *Geol Sci Technology Inf* (2012) 31(3):55–62. doi:10.3969/j.issn.1000-7849.2012.03.008
12. Yang H, Fu JH, Liu XS, Meng P. Accumulation Conditions and Exploration and Development of Tight Gas in the Upper Paleozoic of the Ordos basin. *Pet Exploration Development* (2012) 39(3):295–303. doi:10.1016/s1876-3804(12)60047-0
13. Zhao J, Cao Q, Bai Y, Er C, Li J, Wu W, et al. Petroleum Accumulation: from the Continuous to Discontinuous. *Pet Res* (2017) 2:131–45. doi:10.1016/j.ptlrs.2017.02.001

Conflict of Interest: XW was employed by PetroChina Company Limited Changqing Oilfield Branch.

The remaining authors declare that the research was conducted in the absence of any commercial or financial relationships that could be construed as a potential conflict of interest.

Publisher's Note: All claims expressed in this article are solely those of the authors and do not necessarily represent those of their affiliated organizations, or those of the publisher, the editors and the reviewers. Any product that may be evaluated in this article, or claim that may be made by its manufacturer, is not guaranteed or endorsed by the publisher.